"SURFACTANT-POLYMER INTERACTION IN ENHANCED OIL RECOVERY"

Norman Alban and Jorge Gabitto
Chemical Engineering Department
Prairie View A&M University
P. O. Box 397
Prairie View, TX 77446
409-857-2427

ABSTRACT

The goal of this research is to use the interaction between a surfactant and a polymer for efficient displacement of tertiary oil by improving slug integrity, adsorption and mobility control. Surfactant - polymer flooding has been shown to be highly effective in laboratory-scale linear floods. The focus of this research is to **design an inexpensive surfactant-polymer mixture that can efficiently recover tertiary oil** by avoiding surfactant slug degradation, high adsorption and viscous/heterogeneity fingering.

A mixture comprising a "pseudo oil" with appropriate surfactant and polymer has been used to optimize oil recovery. The physical properties and phase behavior of this system have been determined. A surfactant-polymer slug has been designed to achieve high efficiency recovery by improving phase behavior and mobility control. Recovery experiments have been performed on linear cores. The same recovery experiments have been simulated using a commercially available simulator (UTCHEM). Good agreement between experimental data and simulation results has been achieved.

INTRODUCTION

More than 224 billion barrels of immobile oil remain in U. S. domestic reservoirs. For a number of reservoirs, chemical EOR methods may be the only viable methods for significantly reducing oil saturation in the field.

Capillary forces cause large quantities of oil to be left behind after waterflooding of an oil reservoir. Capillary forces arise from the interfacial tension (IFT) between the oil and water phases that resist externally applied viscous forces and causesthe injected water to bypass the resident oil. The predominant mechanism to recover this oil is lowering the IFT through the addition of suitable chemicals (surfactants). Lower interfacial forces recover additional oil by reducing these capillary forces. This trapping of the resident oil can be expressed as a competition between viscous forces, which mobilize the oil, and capillary forces, that trap the oil.

In practice surfactant injection alone can not achieve sufficient recovery due to several problems, fingering, adsorption, surfactant-soil interactions, etc. Therefore, a more complex process involving different steps is required to fully realize this technique

potential. This recovery process receives different names, but throughout this work wewill use the term micellar-polymer flooding (MP) following Lake[1].

Figure 1 (taken from Lake[1]), shows an idealized version of an MP flooding sequence. The process is applied in the drive mode. The process consists of:

Preflush. A volume of brine to lower salinity is added first. Preflushes range from 0 to 100% pore volume (PV). Sometimes an agent is added to lessen the surfactant retention[2].

MP slug. The main surfactant, cosurfactants, and other chemicals are added later. Slug volumes range from 5 to 20% PV.

Mobility buffer. This fluid is a dilute solution of a water-soluble polymer whose purpose is to drive the MP slug and banked-up fluids towards the production wells. The buffer volumes range from 0 to 100% PV.

Mobility buffer taper. This is a volume of brine that contains dilute polymer added to produce a gradual change in polymer concentration from the mobility buffer concentreation to zero.

Chase water. This fluid is injected to reduce the cost of continuous injection of polymer.

Adequate design of all these different steps requires careful consideration of phase behavior and physical properties of all the chemicals used. A successful MP flood must achieve three things for effective oil recovery[1].

(1). The MP slug should propagate at optimal conditions, especially salinity.

(2). Surfactant concentration should be big enough so that some of it is not retained by permeable surfaces.

(3). The active surfactant should sweep a large portion of the reservoir without excessive dissipation due to dispersion or channeling.

One of the most important variables to achieve the aforementioned conditions is salinity. Lowering the resident salinity is the main purpose of the preflush step. A successful preflush will permit an MP slug to displace oil wherever it goes and will reduce retention and loss of surfactant activity. Several salinity gradient design techniques have been proposed[3,4]. The concept is to dynamically lower the resident salinity to optimal by injecting an underoptimal mobility buffer salinity. Pope et. al.[5] found salinity to be the most important variable controlling the oil recovery process in a series of laboratory experiments.

Mobility control of the MP slug is another critical factor in achieving a successful recovery. Field slugs are relatively small and can not tolerate even a small amount of fingering. Therefore, a slug less mobile than the oil bank it is displacing is sought. Polymer should be added to the MP slug to achieve this goal. The spike portion of the mobility buffer must have a mobility equal or less than the slug.

In order to understand the bases for a successful MP process design a simplified system phase behavior is presented. Surfactant-brine-oil is conventionally illustrated on a ternary diagram[1]. The top apex of the diagram represents the surfactant pseudocomponent, the lower left represents the brine and the lower right represents oil (see Figure 2).

Brine salinity strongly affects the phase behavior. Figure 2 shows a sequence of phase diagrams as salinity is increased. The phase behavior described here has been taken from Nelson and Pope[6]. At low brine salinity, a typical surfactant will exhibit good aqueous-phase solubility and poor oil phase solubility. Thus an overall compositionnear the brine-oil boundary will split into two phases: an excess almost pure oil phase and a microemulsion phase that contains brine, surfactant and solubilized oil. This type of phase behavior is called Winsor type I or type II(-) system. The two phase region is enclosed by a binodal curve. Equilibrium two phase compositions are linked by tie-lines. A especial point (plait) denotes the composition the concentrations in both phases coincide. Above the binodal curve we have only one phase. The tie-lines in II(-) behavior have negative slopes.

For high brine salinities electrostatic forces reduce the surfactant's solubility in the aqueous solution. Therefore, an overall composition, within the two-phase region, will split into an excess brine phase and a microemulsion phase that contains mostof the surfactant and some solubilized brine. The phase environment is called a Winsor type II or a type II(+) system. These behaviors constitute extreme cases. For a range of intermediate salinities a third surfactant rich phase can appear. An overall composition within the three-phase region separates into excesses oil and water rich phases and into a microemulsion whose composition is represented by an invariant point. This phase behavior is called a Winsor III type or a type III system. Over the type III salinity range there is migration of the invariant concentration point M from near the oil apex to near the brine apex. The migration of the invariant point implies essentially unlimited solubility ofoil and brine in a single phase. Several physical properties take extreme values at this critical point. The optimal salinity point can be determined by plotting interfacial tensions in the oil rich and aqueous rich phases versus salinity[7]. The optimal salinity corresponds roughly to the salinity where oil recovery from a core is maximum[1]. Optimal salinities depend upon the nature of the surfactant and the brine pseudocomponents. Adding cosurfactants to the MP slug normally increases the optimal IFT. The notion of optimal salinity is directly related to the phase behavior of MP systems.

SIMULATOR BACKGROUND

UTCHEM, a chemical simulator developed by researchers at the University of Texas at Austin[8], has been used for the simulation program. UTCHEM is a multicomponent, multiphase, three-dimensional compositional with variable temperature simulation model. The basic equations include: mass, pressure and energy balances. The flow equations allow for compressibility of rock and fluids, dispersion and molecular diffusion, chemical reactions, and phase behavior and are complemented by constitutive equations. The model includes options for multiple wells completed either horizontally

or vertically. Aquifer boundaries are modeled as constant potential surfaces or as closed surfaces.

The flow equations are solved using a block-centered finite-difference scheme. The solution method is implicit in pressure and explicit in concentration (IMPES-like). Either one, two-point upstream, or third-order spatial, discretization is used. A brief description of the equations relevant to this research is provided below.

Polymer and Surfactant Adsorption. Polymer and surfactant adsorption can be an important mechanism for a chemical recovery project since it causes retardation and polymer consumption. The retention of polymer molecules in permeable media is due to both adsorption onto solid surfaces and trapping within small pores. UTCHEM uses a Langmuir-type isotherm to describe the adsorption level of these chemicals, which takes into account the salinity, polymer or surfactant concentration, and soil permeability[9]. The adsorption is irreversible with concentration and reversible with salinity. The adsorbed concentration ($\hat{C}_p$) is given by,

$$\hat{C}_p = \min \{ \tilde{C}_p, \frac{a_p (\tilde{C}_p - \hat{C}_p)}{1 + b_p (\tilde{C}_p - \hat{C}_p)} \} \quad (1),$$

where $\tilde{C}_p$ is the overall volume of component k per unit pore volume.

The minimum is taken to guarantee that the adsorption is no greater than the total polymer concentration. Adsorption increases linearly with effective salinity and decreases as follows,

$$a_p = (a_{p1} + a_{p2} C_{SEP}) k^{-0.5} \quad (2).$$

The adsorption parameters a_{p1}, a_{p2} and b_p are found by matching laboratory polymer adsorption data. The effective salinity for polymer (C_{SEP}) is,

$$C_{SEP} = \frac{C_{51} + (\beta_p - 1) C_{61}}{C_{w1}} \quad (3),$$

where C_{51}, C_{61}, and C_{w1} are the anion, calcium, and water concentrations in the aqueous phase and β_p is experimentally determined.

Viscosity. Liquid phase viscosities are modeled in terms of pure component viscosities and the phase concentrations of the organic, water and chemicals,

$$\mu_k = C_{wk} \mu_k e^{\alpha_w (C_{ok} + C_{chk})} + C_{ok} \mu_k e^{\alpha_o (C_{wk} + C_{chk})} + C_{chk} \mu_k e^{\alpha_{ch} (C_{wk} + C_{ok})} \quad (4),$$

where μ_k is the k phase viscosity, C_{ik} is the concentration of component i in phase k, and k = water, oil or chemical.

The α parameters are determined by matching laboratory microemulsion viscosities at several compositions. In the absence of polymer, water and oil phase viscosities are reduced to pure water and oil viscosities. When polymer is present μ_w is replaced by μ_p.

Surfactant/Brine/Oil phase behavior. The surfactant-oil-water phase can be represented as a function of effective salinity once the binodal curve and the tie-lines are described. The phase behavior model in the UTCHEM simulator uses Hand's rule[10], and is based on the work by Nelson and Pope[7], among others. The effective salinity increases with the divalent cations bound to micelles (Hirasaki[11]) and decreases as the temperature increases for anionic surfactants.

The formulation of the binodal curve using Hand's rule[10] is assumed to be the same in all phase environments. Hand's rule is based on the empirical observation that equilibrium phase concentration ratios are straight lines on a log-log plot scale. Figures 3a and 3b show a type II(-) ternary diagram and its corresponding Hand plot. The binodal curve is computed from,

$$\frac{C_{3j}}{C_{2j}} = A\{\frac{C_{3j}}{C_{1j}}\}^B, \text{ with } j = 1,2, \text{ or } 3 \qquad (5),$$

where A and B are empirical parameters. For a symmetric binodal curve where B = -1 all phase concentrations are calculated explicitly in terms of oil concentration C_{2j}.

$$C_{3j} = 0.5\left[- A\ C_{2j} + \sqrt{(A\ C_{2j})^2 + 4\ A\ (1 - C_{2j})}\ \right], \text{ for } j = 1,2, \text{ or } 3 \qquad (6).$$

EXPERIMENTAL PART

Several chemical systems were tested to determine oil recovery potential for an oil mixture designed with a viscosity of approximately 10 cp. The tests included phase behavior observations, viscosity measurements, interfacial tension measurements, and a linear oil recovery experiment. The suggested chemical system is composed of a surfactant (petroleum sulfonate), co-surfactant (2-methyl, 1-propanol), and a high molecular weight polyacrylamide.

MATERIALS:

Oil. Two oil mixtures were formulated to obtain a paraffin-based oil with an approximate viscosity of 10 cp at ambient temperature. Oil 1 consisted of 68% motor oil (SAE 30 non detergent motor oil) and 32% decane. Oil 2 was 66.5% Soltrol 220 (isoparaffinic oil from Phillips Petroleum Co) and 33.5% SAE 30 motor oil. The viscosity of Oil 2 is 11.6 cp at 23 °C and 9.88 cp at 30 °C. The viscosity of Oil 1 is 9.32 cp at 30 °C and should be slightly higher at ambient temperature.

Surfactant/Co-surfactant. The co-surfactant used for these studies was 2-methyl, 1-propanol (isobutyl alcohol or IBA). Alcohol molecules are incorporated in surfactant micelles and change surfactant solution properties (such as viscosity, partitioning, and solubility). Two petroleum sulfonate surfactants from Witco Corporation were tested. Table 1 summarizes surfactant information. All surfactant/co-surfactant mixtures were prepared by wt%/wt% in different concentration sodium chloride solutions. The alcohol was always used at the same concentration as the surfactant.

Polymer. The polymer is a high-molecular-weight hydrolyzed polyacrylamide, Alcoflood 1275, from Allied Colloids, which is available in powder form. This polymer is anionic, and its average molecular weight is 22×10^6 dalton.

EQUIPMENT AND PROCEDURES:

Viscosities were measured with a Brookfield Cone and Plate viscometer. IFTs (interfacial tension measurements) were determined with a spinning drop tensiometer.

Phase behavior of the surfactant/brine/oil system was determined by mixing equal volumes of aqueous and oil phases in tubes made from 10 cc pipets which have had the tips sealed to prevent fluid leaks. Volumes can be read to 0.1 cc from the marking on the pipets. To determine optimal salinity and the 3-phase salinity region, a series of tubes is prepared with different salt concentrations. The tubes are shaken and allowed to equilibrate. If surfactant remains in the aqueous phase after equilibration, the salinity is under optimum and is designated II(-). If the surfactant partitions into the oil phase, salinity is over optimum and is designated II(+). If three phases form (oil, brine, and middle phase), the behavior is designated III.

Oil Recovery. An oil recovery experiment was conducted in a Berea sandstone core plug 1.5 in. in diameter and 9.5 in. long. Core permeability was 506 md at 100% water saturation. Porosity was 23.3%. The core was initially saturated with non damaging brine, then oil was flooded to residual water saturation, and saturated with water to residual oil saturation before conducting the chemical flood experiment. Figure 4 shows the Hassler sleeve apparatus and experimental equipment used in the oil recovery test.

RESULTS

Phase Behavior and Interfacial Tension

A quick screen test using Oil 1 and Witco EOR 2094 Surfactant to determine salinity effect on 3-phase formation indicated that a middle phase would form around the 1% NaCl concentration region. Very low IFT values were measured between this oil and surfactant in 1% NaCl, as shown in table 2.

In the case of Oil 2 and Witco EOR 2095 a phase tubes experiment showed 3-phase behavior for salinities between 1.1 and 1.45% NaCl. Figure 5 shows the phase volumes, and Figure 6 shows the solubilization parameters for this system. Optimum salinity was approximately 1.39% NaCl. The presence of polymer in the solution did not change the optimum salinity. The optimum salinity changed slightly as the ratio of oil components changed. An oil mixture of 87.5% Soltrol 220 and 12.5% motor oil had an optimum salinity of 1.22%. Optimum salinity also decreased as the concentration of surfactant decreased. A 1% surfactant solution with Oil 2 showed a 3-phase region from 0.75% NaCl through 1.2% NaCl. A 0.5% surfactant solution produced a small third phase around 1% salinity. IFT values between Oil 2 and 3% EOR 2095 at optimum salinity were not as low as the IFTs between Oil 1 and 3% EOR 2094.

It was found that Alcoflood 1275 polymer develops the highest viscosity in low salinity brine. Adequate viscosity is generated, however, by a 1,000 ppm polymer solution when

prepared in a sodium chloride solution at optimal salinity for the surfactant/oil mixtures under study.

Oil Recovery

Oil recovery in a linear flow configuration was conducted using the following fluids:

- Brine 1.4% NaCl
- Oil 66.5% Soltrol 220, 33.5% non detergent motor oil SAE 30
- Surfactant 3% Witco EOR 2095, 3% 2-methyl, 1-propanol in 1.39% NaCl, and 1,000 ppm 1275 polyacrylamide.
- Polymer 1,000 ppm Alcoflood 1275 polyacrylamide in 1.4% NaCl
- Chase brine 1.4% NaCl

The planned chemical injection volumes were 0.2 PV or less of surfactant and 1.0 PV or less of polymer. Actual injected PVs were 0.20 for surfactant and 0.77 for polymer. The fluids were injected at a rate of 10 ft/day. Note that this is not a salinity gradient experiment. The system, however, produced over 90% of the oil remaining after waterflood as shown in Figure 7. Some emulsions were produced toward the end of the oil production. They were broken by addition of a small amount of 2-propanol(IPA). These results indicate that the chemical system appears to have adequate oil recovery capabilities.

Simulation Results

The UTCHEM simulator has several interesting features that can be used to thoroughly study the chemical flooding process. Saturation, concentration, viscosity, IFT and other property profiles can be obtained as results of appropriate simulation runs. The integration domain is divided in blocks. We used eleven blocks in the x direction in our coreflood studies. The simulator also calculates the system phase behavior block by block, reporting a phase behavior profile that can be compared with the phase behavior information obtained using other properties.

Typical results for our simulations are shown in Fig. 8. Effective salinity is plotted versus the geometrical coordinate x. The effective salinity concentration profile decreases monotonically from the core entrance to the core exit. The first four blocks have an effective salinity concentration higher than the upper limit,therefore, a II(+) behavior is expected for these blocks. A microemulsion phase will be at equilibrium with an aqueous phase. Blocks 5 to 8 are within the upper and lower effective salinity limits, therefore three phases will be at equilibrium in thoseblocks. Block 5 has been reported to behave as a type 4 phase behavior. According to the UTCHEM simulator convention, type 4 represents the equilibrium in the left lobe (II+) of a type III region. Blocks 9 to 11 are located below the lower salinity limit, therefore, a II(-) behavior is expected for these blocks. A microemulsion phase will be at equilibrium with an oil rich phase.

Figs. 9 through 11 show the variation of different properties along the core plug. The variation of these properties can beinterpreted using the phase behavior discussed above.

The relationship between these properties and the oil recovery efficiency can also be determined from the study of these figures. A zero value for any property in any of the three phases means that this phase is not present in the block under consideration.

Fig. 9 shows the variation of viscosity with position. Oil viscosity is zero for the first four blocks and aqueous phase viscosity is zero for the last three. This result is in agreement with the phase behavior discussed above. The viscosity plays a big role in the efficiency of the recovery process. The aqueous phase is ten times less viscous than the oil phase (1 cp to 10 cp). Therefore, polymer is added to the mobility buffer to avoid fingering. This figure reflects the situation after injection of 0.5 PV. The viscosity of the aqueous and microemulsion phases is higher than the oil phase viscosity for blocks 1 to 7. Blocks 8-11 present higher oil phase viscosity. Other simulation results ,not presented here, showed that the oil bank moves towards the production part of the core as the injected volume increases. In conclusion the oil bank is pushed towards the production well by the more viscous aqueous and microemulsion phases. This situation can be observed in Fig. 10. The oil saturation is zero or nearly zero for the first five blocks and increases very rapidly for the blocks 6 to 11. The microemulsion phase saturation profile presents a maximum at block 6 decreasing for blocks 7 to 11. Aqueous phase saturation decreases from blocks 1 to 7. Water is being trapped into the microemulsion phase. Then, it disappears in blocks 8 to 11.

Fig. 11 shows values of interfacial tension (IFT) within the core plug. Decimal logarithm of IFT is plotted vs. X direction. There are two possible interfaces for this system microemulsion/water and microemulsion/oil. The IFT value is different for both interfaces when three phases are present, blocks 6 to 8. Equal IFT values imply than only two phases are present, blocks 1 to 5 and 9 to 11. The figure also shows that from block 1 to 10 the IFT is significant smaller than the pure water IFT value (+1.65 mN/m). These low values are produced because the effective salinity values are everywhere within close proximity of the optimal salinity range. This figure is an extreme example of the reduction in IFT reached through adjustment of the effective salinity. The high recovery achieved in this case, even for a high viscous oil shows the potential of chemical flooding methods to recover residual oil.

Figure 12 shows a comparison between experimental data and simulation results for oil production. There is good agreement for all values between simulation results and experimental data. The biggest discrepancy occurs for small values of PV. The calculated results predict higher recovery than the experimental data. For medium and high volumes the results are practically the same. This figure shows that the simulation results can be used with reasonable confidence to design these processes.

CONCLUSIONS

Fluid systems were evaluated for oil recovery studies in this project. The selected chemicals and fluids allow adjustments in fluid properties to study surfactant-polymer interactions under variable but controlled conditions. These properties were successfully tested in linear flooding experiments. Simulation results agreed satisfactorily with experimental data for linear floods. Simulation results allowed us a thorough evaluation

of the properties affecting recovery efficiency. Phase behavior was determined primarily by the effective salinity value. A flooding experiment conducted within a small range of optimal salinity can achieve very low IFT and increased "solubility" of the oil in a microemulsion phase. Mobility control was also important. The presence of a mobility buffer with a viscosity equal or higher than the mobilized oil increased significantly the recovery efficiency. In conclusion these experiments and calculations showed the potential of micellar-polymer flooding as a tertiary oil recovery process.

ACKNOWLEDGEMENTS

Department of Energy support through subcontract G4S60336, prime contract number: DE-AC22-94PC91008 is kindly acknowledged.

REFERENCES

1. Lake, L. W. "Enhanced Oil Recovery," *Prentice Hall*, New Jersey, 1989.
2. Holm, , L. W. "Effect of Oil Composition on Miscible-Type Displacement by Carbon Dioxide," *Society of Petroleum Engineering Journal*, **22**, 87-98(1982).
3. Chou, S. I. and Shah, D. O. "Optimal Salinity of Polymer Solution in Surfactant-Polymer Flooding Processes," in Surface Phenomena in Enhanced Oil Recovery, edited by D. O. Shah, Plenum Press, New York and London, 1981.
4. Hirasaki, G. J., van Domselaar, H. R. and Nelson, R. C. "Evaluation of the Salinity Gradient Concept in Surfactant Flooding," *Society of Petroleum Engineering Journal*, **23**, 486-500(1983).
5. Pope, G. A., Ben Wang. and Kerming Tsaur, F. G. "A Sensitivity Study of Micellar-Polymer Flooding," *Society of Petroleum Engineering Journal*, **19**, 357-358(1979).
6. Nelson, R. C. and Pope G. A. "Phase Relationships in Chemical Flooding," *Society of Petroleum Engineering Journal*, **18**, 325-338(1978).
7. Reed, R. L. and Healy, R. N. "Some Physico-Chemical Aspects of Microemulsion Flooding: A Review," Improved Oil Recovery by Surfactant and Polymer Flooding, D. O. Shah and R. S. Schecter editors, Academic Press, New York, 1977.
8. Pope G. A. and Nelson R. C., "A Chemical Flooding Compositional Simulator," *Society of Petroleum Engineering Journal*, **18**, 339-354(1978).
9. Hirasaki, G. J. and Pope G. A. "Analysis of Factors Influencing Mobility and Adsorption in the Flow of Polymer Solution Through Porous Media," *Society of Petroleum Engineering Journal*, **14**, 337-346(1974).
10. Hand, D. B. "Dineric Distribution: I. The Distribution of a Consolute Liquid Between Two Immiscible Liquids," J. of Physics and Chem., **34**,1961-2000(1939).

11. Hirasaki, G. J. "Application of the Theory of Multicomponent, Multiphase Displacement to Three-Component, Two-Phase Surfactant Flooding," *Society of Petroleum Engineering Journal*, **21**, 191-204(1981).

TABLE 1. Petroleum Sulfonates from Witco Corporation

	EOR 2094	EOR 2095
	Petroleum Sulfonate	Petroleum Sulfonate
Equivalent Wt.	422	416
% Active	50.6	50

Table 2. IFT as a function of time for Oil 1 and EOR 2094

3% 2094, 3% IBA, 1.0% NaCl	
SAE 30/32% Decane	
Time (min.)	**IFT (mN/m)**
0	0.00565
2	0.00458
5	0.00559
10	0.00560
15	0.00582
25	0.00323
	0.00341
	0.00326

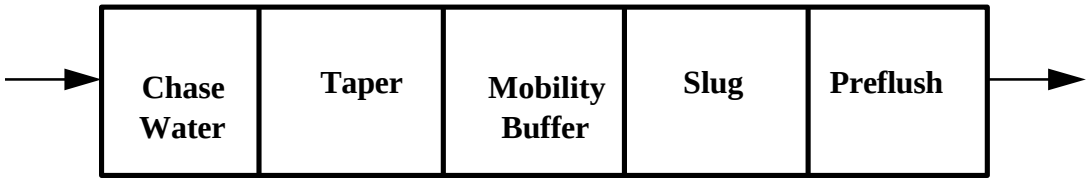

Mobility Buffer	Slug	Preflush
250-2500 g/m3 polymer	1-20% Surfactant	Electrolyte
0-1% alcohol	0-5% Cosurfactant	(Na, Ca, etc.)
Stabilizers	0-5% Alcohol	Sacrificial
Biocide	Polymer	Chemicals
0-100%PV	5-20%PV	0-100%PV

Fig. 1. Cross section of a typical micellar-polymer flood.

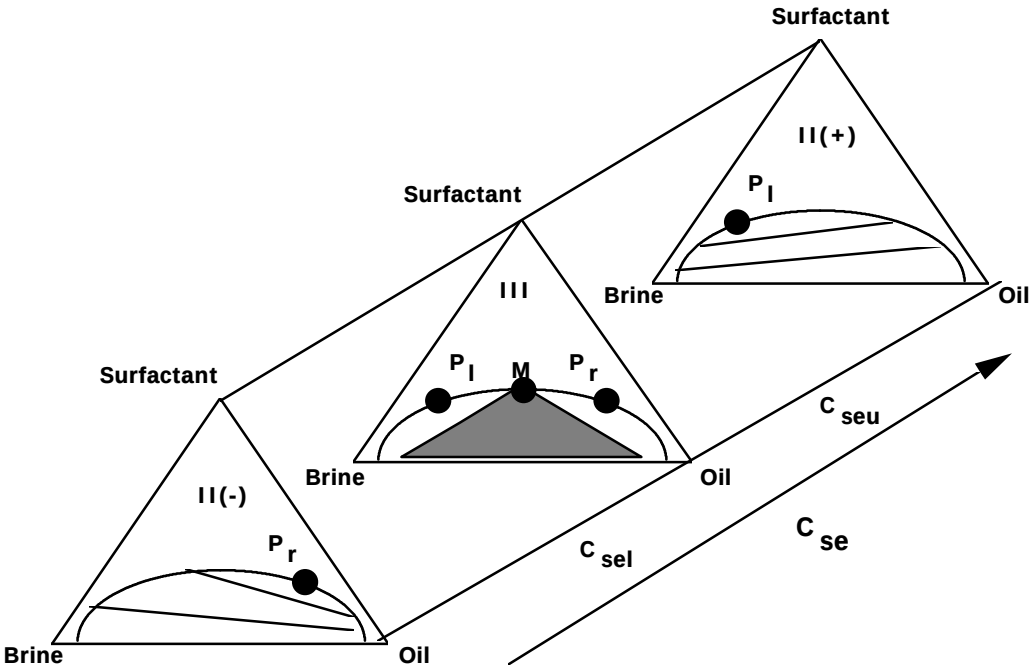

Fig. 2. Ternary diagram representation of micellar-polymer phase behavior.

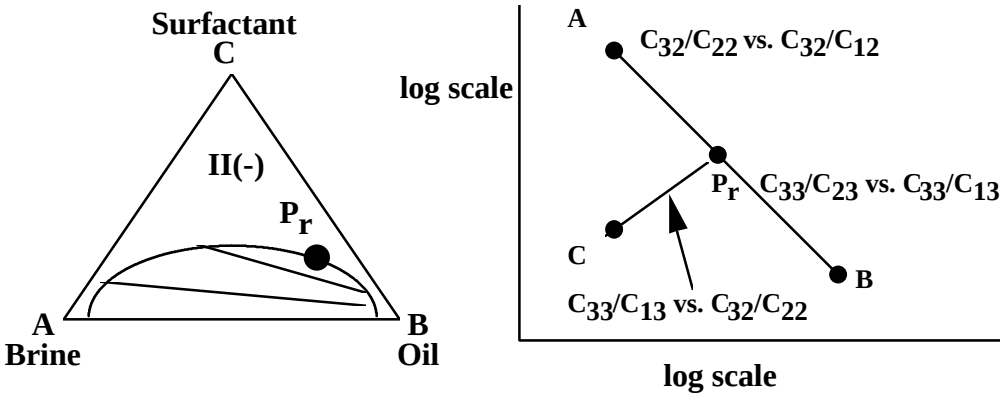

Fig. 3. Correspondence between a ternary diagram and a Hand plot.

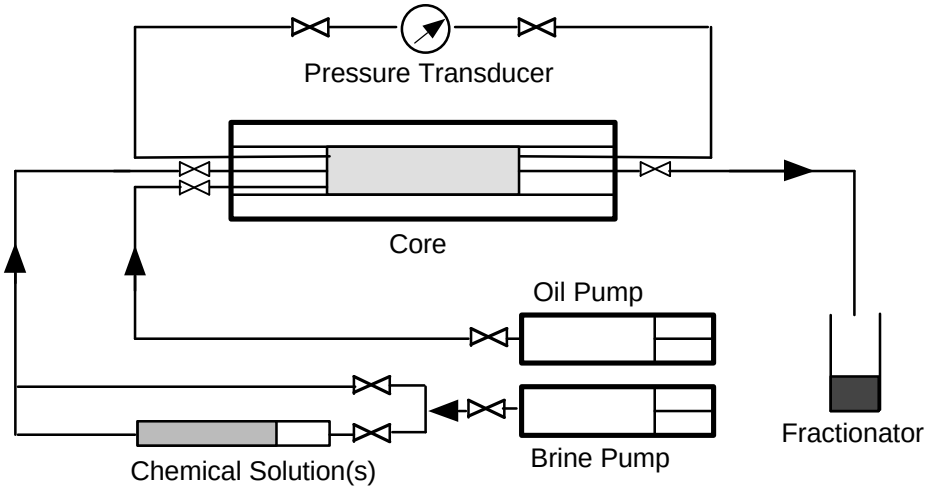

Figure 4 Coreflood apparatus

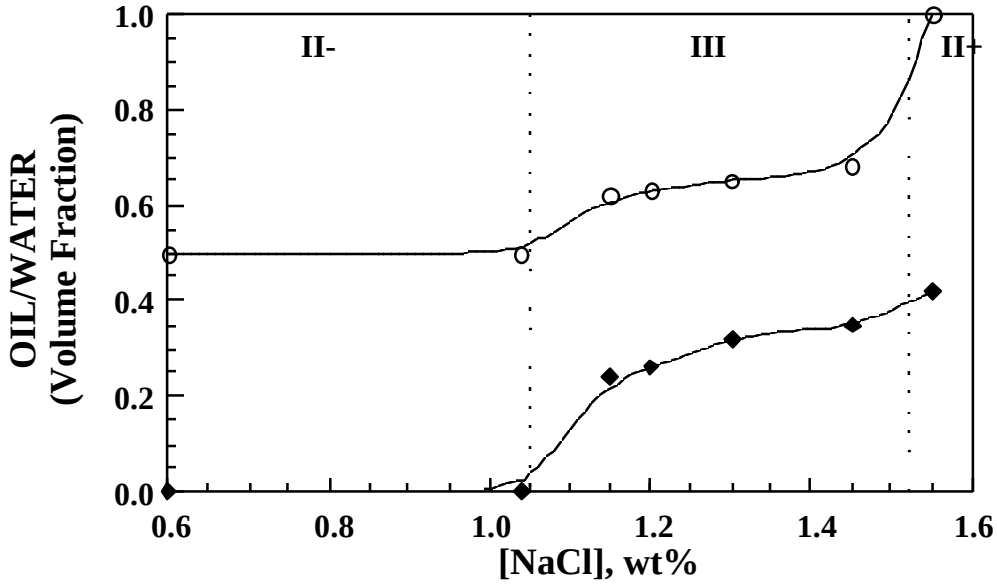

Figure 5. 2-phase and 3-phase regions as a function of increasing salt concentration for the Witco EOR 2095 surfactant and Oil 2.

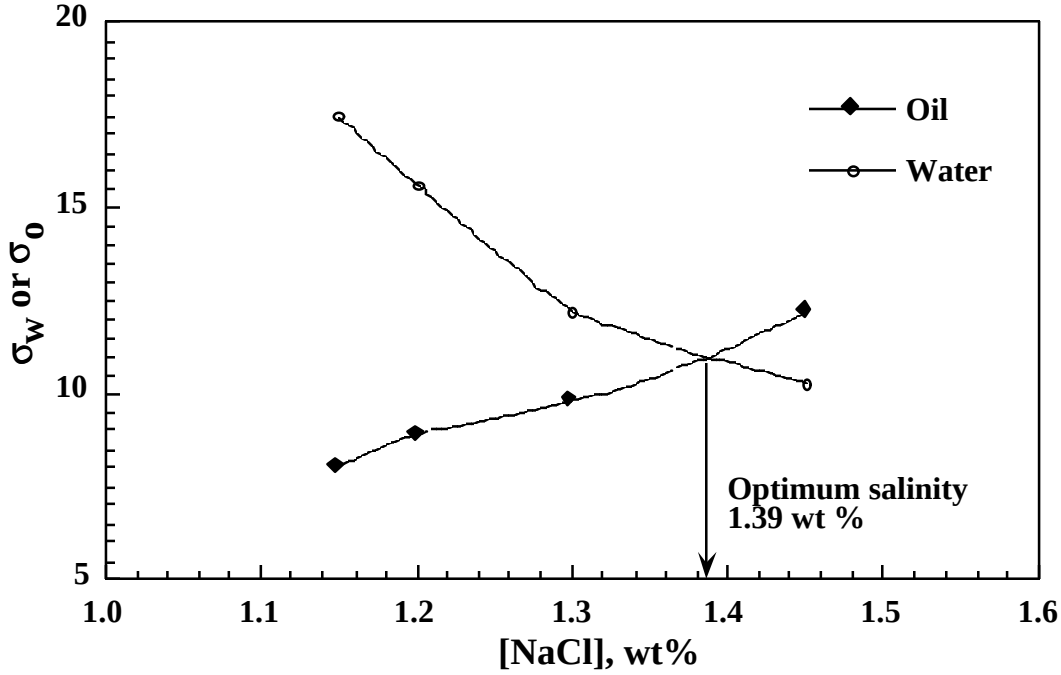

Figure 6. Oil and water solubilization parameters as a function of salinity. Optimum salinity for the system is at a concentration of approximately 1.39% NaCl.

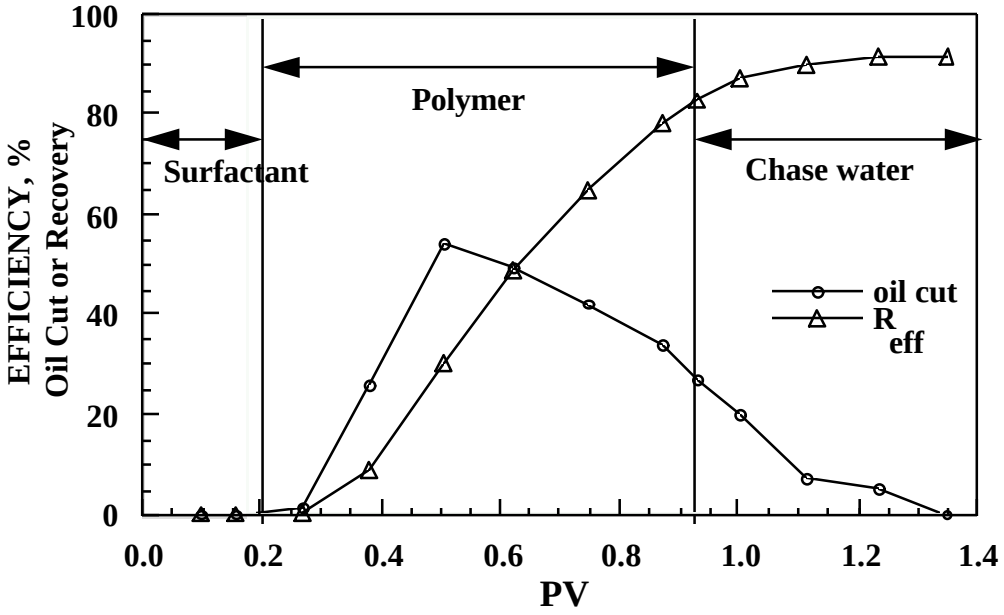

Fig. 7. Oil cut and recovery efficiency as a function of fluid injected for an oil recovery experiment in a Berea sandstone core plug.

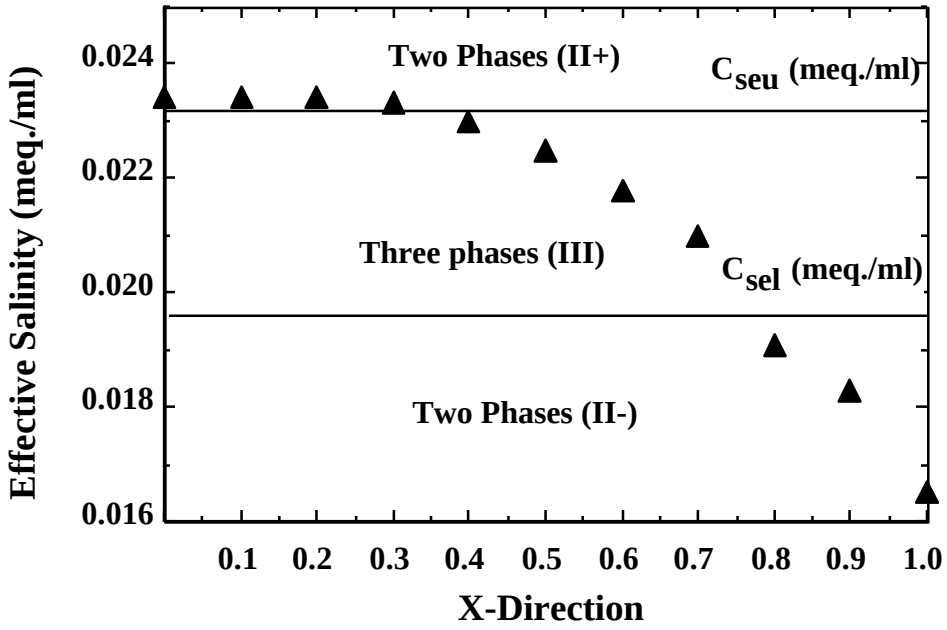

Fig. 8. Relationship between phase behavior and effective salinity along the Berea core plug.

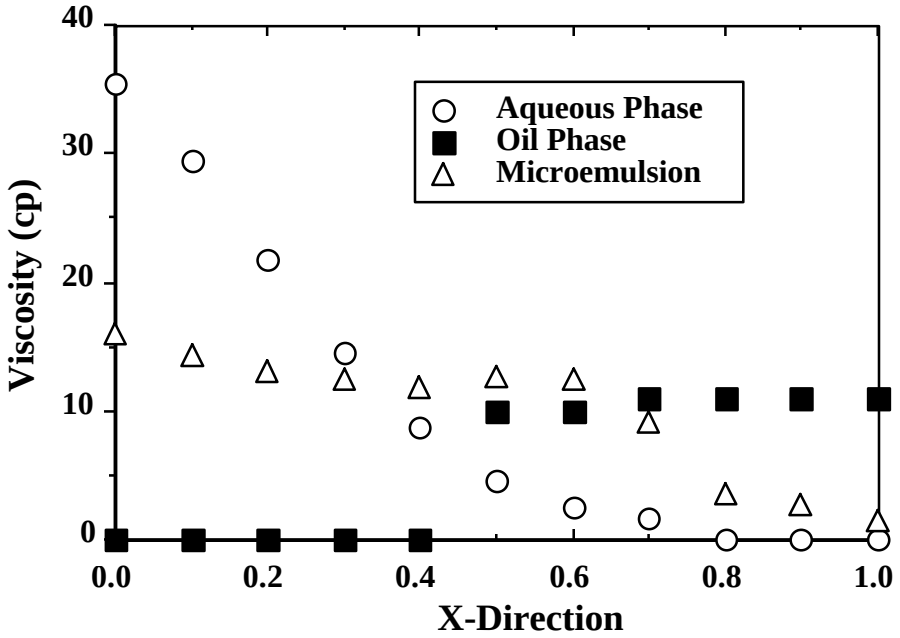

Fig. 9. Viscosity change along the Berea core plug.

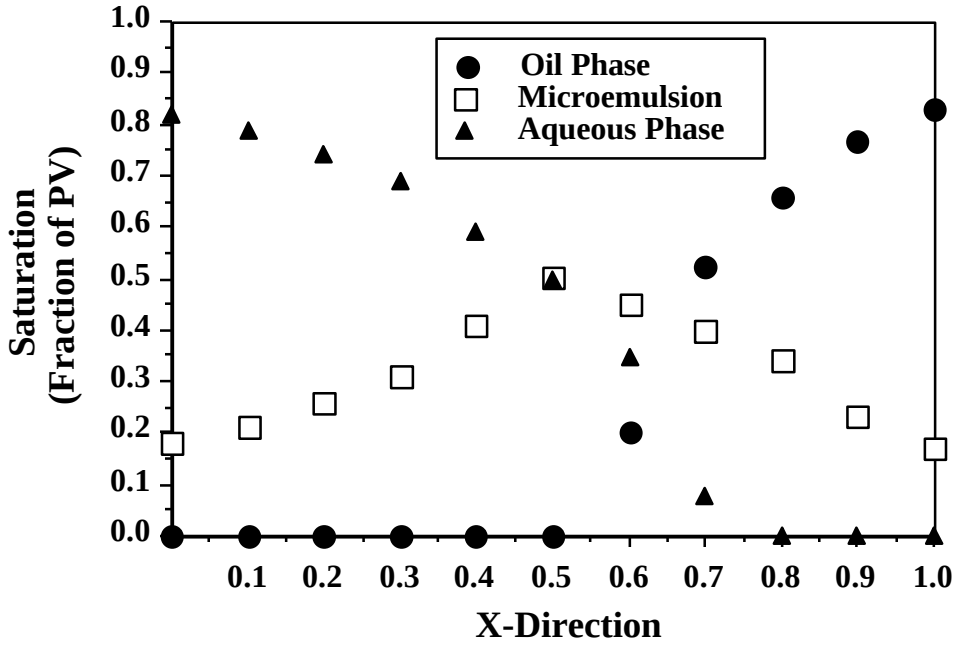

Fig. 10. Phase saturations inside the Berea core plug.

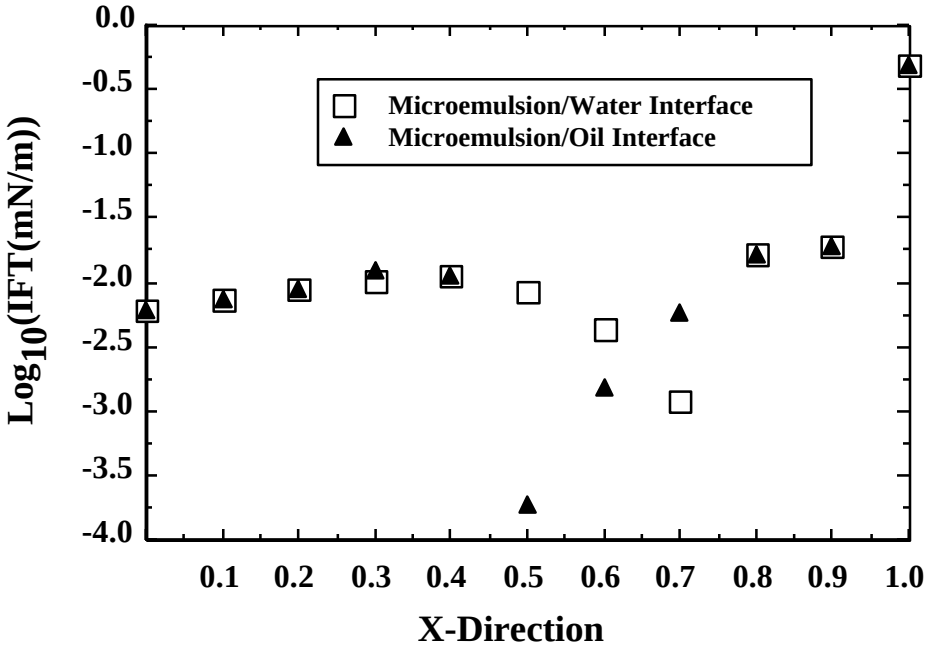

Fig. 11. Interfacial tension (IFT) along the Berea core plug.

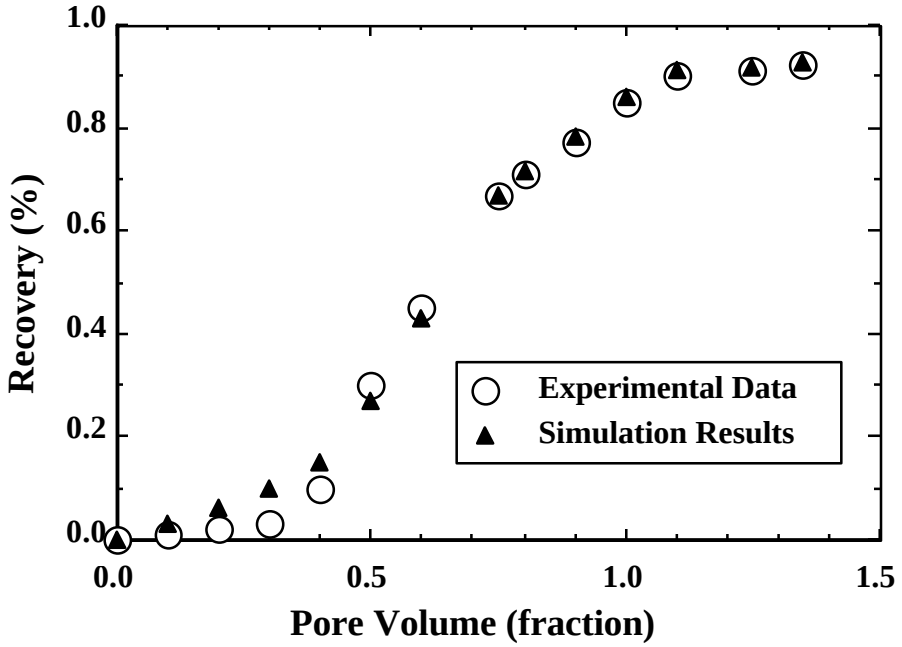

Fig. 12. Comparison of experimental data and simulation results.